Real-time Model Predictive Control of a Wastewater Treatment Plant based on Machine Learning

A. Bernardelli*, P. Gelli**, A. Manzini*, S. Marsili-Libelli***, S. Stancari*, S. Venier**

* EnergyWay srl andrea.bernardelli@energyway.it; alberto.manzini@energyway.it; simone.stancari@energyway.it

** Gruppo Hera spa paolo.gelli@gruppohera.it; stefano.venier@gruppohera.it

*** University of Florence (ret.) stefano.marsililibelli@unifi.it

Abstract: In wastewater treatment two separate goals should be jointly pursued: nutrient removal and energy conservation. An efficient controller performance should cope with process uncertainties, seasonal variations and process nonlinearities. This paper describes the design and testing of a model predictive controller (MPC) based on neuro-fuzzy techniques, capable of estimating the main process variables and provide the right amount of aeration to achieve an efficient and economical operation. The algorithm has been field-tested on a large-scale municipal WWTP of about 500.000 PE with encouraging results in terms of better effluent quality and energy savings.

Keywords: Machine learning; Artificial Intelligence; Neuro-Fuzzy computing; Nutrient Removal; Model Predictive Control; Real-time Control

Introduction

The goal of this study is the design and engineering of a real-time controller for nutrient removal, based on artificial intelligence (AI). The Wastewater Treatment Plant (WWTP) process scheme is shown in Figure 1, where the dissolved oxygen (DO) set-point DO_{sp} and the recycle flow Q_r are determined on the basis of the future nutrient changes estimated by the artificial intelligence engine (AIE). The MPC manipulates these variables to reduce the amount of output total nitrogen and to minimise the energy consumption. The artificial intelligence engine predicts the future evolution of both ammonia and nitrate and on this basis the model predictive controller determines the DO set-point and the internal recycle.
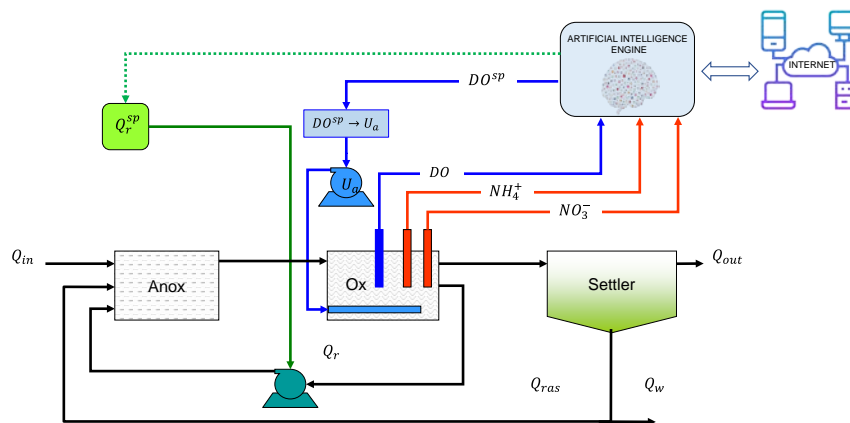
Figure 1 Process scheme of the WWTP to which the MPC is applied.

The observed variables in this control scheme are the dissolved oxygen (DO) together with the Nitrogen species NH_4^+ and NO_3^- in the oxidation tank. The controller outputs are the DO set-point and the internal recycle Q_r expressed as a percentage (0 – 100%) of the maximal allowable flow. The latter arrangement is due to the fact that the recycle pump operates at a fixed regime, so the percentage represents the fraction of the ON time in each time frame.

Material and Methods

The WWTP from which the data were acquired and which is being used as a test plant is the municipal plant of the city of Modena, in Northern Italy. It consists of a conventional nitrification/denitrification plant, as shown in Figure 1, with a capacity of about 500,000 PE.

The process instrumentation consists of a Dissolved Oxygen meter and a nutrient sensor (Hach, Endress+Hauser). These field measurements are routed to the plant SCADA for real-time operation. An encrypted connection between the plant and the Energy Way centre was been created to allow prototypal test. This arrangement enables specific clients to access the controller through LAN. Through VPN encrypted tunnelling, clients can mount directories on the controller as NFS folders and obtain services directly from the controller, enabling fast analysis iteration and maintenance.

Communication between the centre and the plant SCADA is based on the Modbus protocol over TCP/IP, physically linking the controlling machine to the PLC-front-end with an Ethernet patch cable, enabling peer-to-peer IP communication.

The process variables are sampled at regular intervals $\delta = 5$ min and the prediction and control horizons were suitably defined as α and β multiples of δ respectively, which cannot be specified here for industrial confidentiality. The AI components of the MPC were trained and validated using plant data spanning over one year of operation.

The proposed model predictive controller (EW stands for Energy Way) is shown in Figure 2 where in the lower block a set of neuro-fuzzy networks forecasts the relevant process variables α steps ahead, while the upper block implements a heuristic search procedure to select the most appropriate value of the DO set-point β steps ahead.
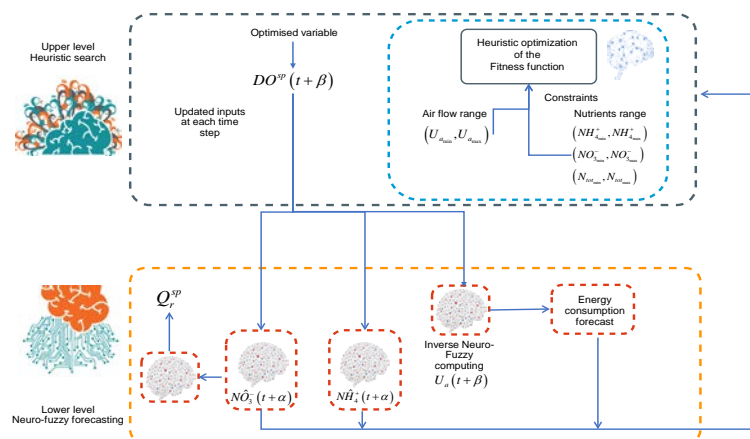

Figure 2 General scheme of the neuro-fuzzy model predictive controller, referred to as EW. The prediction (α) and control (β) horizons are multiples of the sampling interval δ.

It consists of two main parts: the prediction of the future process variables (lower block) and the heuristic search of the "best" input to be applied at the next step (upper block). Unlike many industrial processes where an approximating linear model can be obtained, WWTP is a highly nonlinear, time-varying process. For this reason *ad-hoc* versions of MPC have been devised (Marsili-Libelli and Giunti, 2002; Hong and Bhamidimarri, 2003; Holenda et al., 2008; O'Brien et al., 2011; Han et al., 2014; Yang et al., 2014; Francisco et al., 2015; Mulas et al., 2015; Foscoliano et al., 2016; Goldar et al., 2016; Haimi et al., 2016; Marsili-Libelli, 2016; Han et al., 2017).

Another aspect of WWTP management, is the harmonisation of two control objectives to balance the effluent quality requirements with the energy conservation (Flores et al., 2007; Hakanen et al., 2013; Han and Qiao, 2014; Mustapha et al., 2018; Qiao et al., 2018; Torregrossa et al., 2018). In our controller, shown in Figure 2 the predictive section (lower block) is implemented as a set of neuro-fuzzy networks (Jang, 1993; Jang et al., 1998) further modified by Marsili-Libelli, (2016) and Bartoletti et al., (2018) while the predictive controller (upper block) is based on a heuristic search which selects the best future air flow $U_a^*(t+\alpha)$ as the one which yields the DO value closest to the future set-point $DO_{sp}^*(t+\alpha)$, by testing an array of input values. In details, the neuro-fuzzy networks shown in Figure 3 forecast the nutrient concentrations at α steps ahead, while Figure 4 shows how this information is repeatedly used by the heuristic search engine to compute the best air flow, as described earlier. So while the prediction horizon is α steps ahead, the control horizon is β step ahead for the DO set-point and the air flow, with β < α.
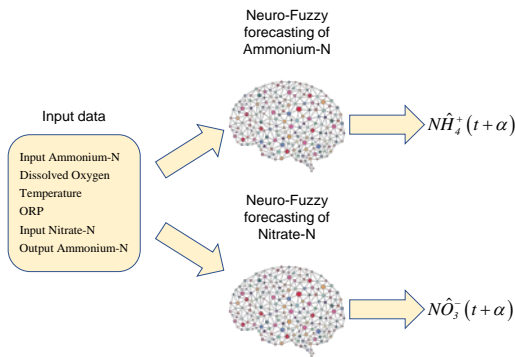
Figure 3 Neuro-fuzzy networks to predict the future outputs (lower block of Figure 2).
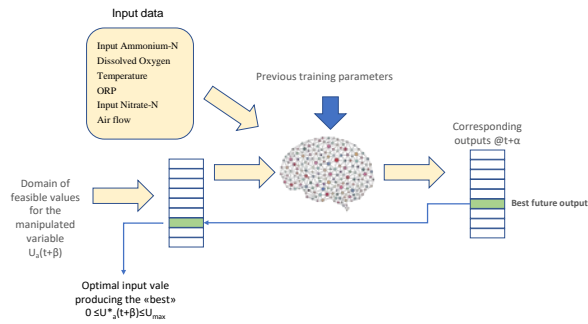
Figure 4 Inverse network to select the best input by heuristic search (upper block of Figure 2).

The prediction accuracy is assessed through the following performance indexes

$$MAE \ (Mean \ Absolute \ Error) = \frac{1}{n}\sum_{i=1}^{n}\left|\hat{y}_i - y_i\right| \quad RAE \ (Relative \ Absolute \ Error) = 100 \times \frac{1}{n}\sum_{i=1}^{n}\left|\frac{\hat{y}_i - y_i}{y_i}\right| \ , \tag{1}$$

where y represents the actual generic variable and $\hat{y}$ its estimate. The inverse network of Figure 4 computes the next DO set-point at each time step by minimising the following weighted sum of process variables as the following objective function which takes into account both the predicted process variables (Nitrogen species) and the energy consumption, represented by the blower energy.

$$DO_{sp}^*(t+\beta) = \min_{DO_{sp}} \left[\begin{array}{l} \gamma_1 \dfrac{N\hat{H}_4^+(t+\alpha)+N\hat{O}_3^-(t+\alpha)}{\overline{N}_{tot}} + \gamma_2 \dfrac{E(t+\beta)}{\overline{E}} + \\[2mm] \gamma_3 \dfrac{DO_{sp}(t+\beta)-DO_{sp}(t)}{\overline{DO}_{sp}} + \rho_1 \dfrac{N\hat{H}_4(t+\alpha)}{\overline{NH}_4} + \\[2mm] \rho_2 \dfrac{N\hat{O}_3(t+\alpha)}{\overline{NO}_3} + \rho_3 \dfrac{\hat{N}_{tot}(t+\alpha)}{\overline{N}_{tot}} \end{array} \right]$$

where

$N_{tot} = NH_4^+ + NO_3^-$

$\gamma_1, \gamma_2, \gamma_3, \rho_1, \rho_2, \rho_3 = weighting \ factors$; $E = blower \ energy$

$\overline{\Box} = average \ value$; $\alpha = prediction \ horizon$; $\beta = control \ horizon$

(2)

While the constraints with the γ weights are always active, those with the ρ coefficients are engaged whenever the pertinent variable activates its constraint, namely

$$\rho_1 \neq 0 \quad if \quad N\hat{H}_4(t+\alpha) \geq NH_4^*$$
$$\rho_2 \neq 0 \quad if \quad N\hat{O}_3(t+\alpha) \geq NO_3^*$$
$$\rho_3 \neq 0 \quad if \quad \hat{N}_{tot}(t+\alpha) \geq N_{tot}^* \tag{3}$$

with $NH_4^*, NO_3^*, N_{tot}^*$ *fixed threshold values*

The recycle flowrate is then updated according to the forecasted process variables

$$Q_r(t+\beta) = Q_r(t) + \frac{N\hat{O}_3^-(t+\alpha) - N\hat{O}_3^-(t)}{N\hat{O}_3^-(t)} \quad \Rightarrow \quad \begin{cases} Q_r(t+\beta) = \min(Q_r(t+\beta), 100) \\ Q_r(t+\beta) = \max(60, Q_r(t+\beta)) \end{cases} \tag{4}$$

Results and Discussion

The estimated process variables at the end of the prediction horizon (t, t+α) provided by the trained neuro-fuzzy predictors are shown in Figure 5 while the improvement in effluent quality and energy saving are shown in Figure 7 and in Table 1.
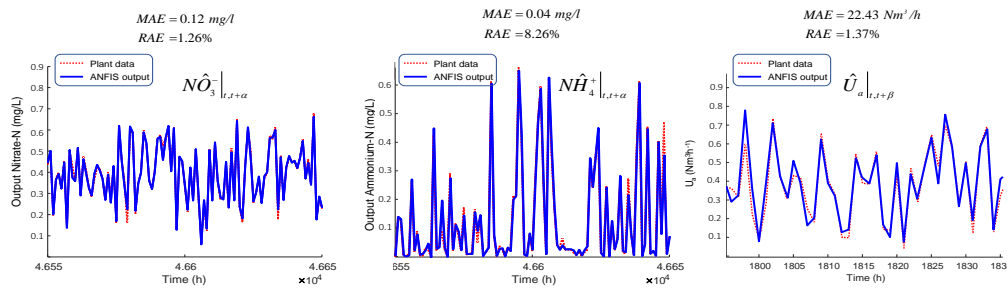
Figure 5 Preliminary off-line prediction of the process variables at time t+α for the nutrients and at t+β for the air flow provided by the trained neuro-fuzzy networks. Normalised values are shown for confidentiality.

A sensitivity assessment was then performed on the model by observing the variations of the output variables (NH_4^+, NO_3^-) caused by a ±20% variation in DO. Figure 6a shows that a positive DO variation of 20% produces a NH_4^+ decrease in 95.8% of the cases (red bars), while a -20% DO variation results in an increase of NH_4^+ in 96.1% of the times (blue bars). Likewise, Figure 6b shows that a +20% DO increase is followed by an NO_3^- increase in 91.7% of the cases, while a -20% DO decrease results in a lower NO_3^- in 92.3 % of the times. The spread in the response is due to the influence of other process conditions.
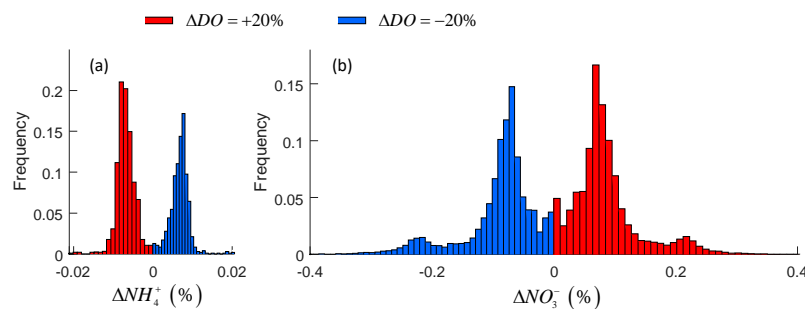
Figure 6 Sensitivity assessment of the predictive model of Figure 3. The ammonium-N variations in response to a 20% change in DO are shown in (a), while (b) shows the corresponding changes in

nitrate-N. Notice the inverted response of the two output variables.

After testing the consistency of the predictions via sensitivity analysis the proposed MPC has been compared with the conventional controller (CC) previously in operation. The total Nitrogen (N_{tot}) comparison of Figure 7 shows that the EW controller, operating between samples 190 and 300, can keep the output N_{tot} lower than the conventional one.
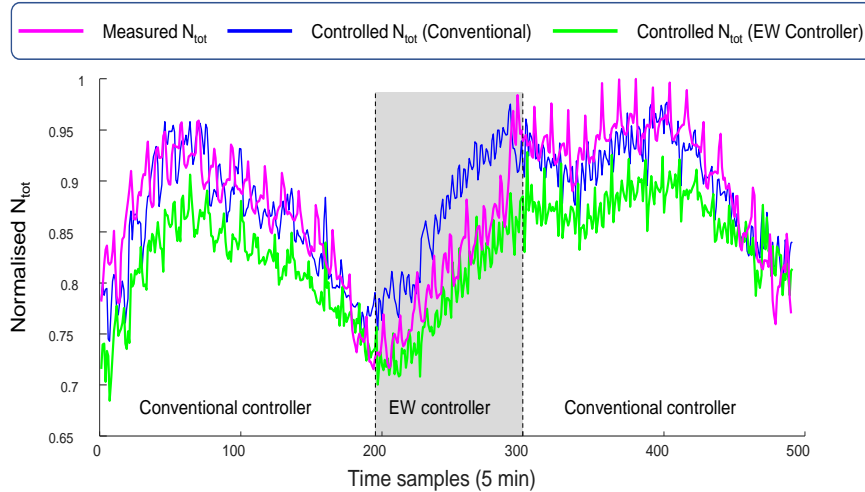
Figure 7 Comparison of total-N output with the conventional and EW controller, operating between samples 190 and 300 (shaded area) corresponding to the period of test in March 2019. A lower N_{tot} output was obtained by the EW controller.

Based on this encouraging result, Table 1 shows the improvement obtained with the EW controller after an extended run in March 2019.

Table 1 Performance improvement achieved by our predictive controller (EW) over the conventional controller (CC) represented by the shaded area in Figure 7.

	Measured averages				Estimated average
	Ammonium-N	Nitrate-N	Total-N	Air Flow	Electric power
Δ(EW-CC)	+2.8%	-7.6%	-5.1%	-10.7%	-10.4%

Two more test runs are now examined, each optimised according to a differing objective. In the first test the emphasis was placed on the effluent quality during a high-load period and the results are shown in Figure 8.

In Figure 8a the DO set-point varies according to the predicted treatment requirements, computed by the forecasting engine of Figure 4, and the DO controller operates in such a way to maintain the DO level close to its set point. Figure 8b shows the corresponding airflow variations, providing more air flow whenever the organic load increases. In particular it can be seen that around samples 1500 and 3400 the DO set-point was raised to cater for the increased treatment demand. The other airflow fluctuations are a consequence of the controller reaction to the varying load, which requires differing level of air flow to track the DO set-point. Figure 8c shows that the predicted N_{tot} is very close to the measured value at all times. The reliability of the forecasting engine of Figure 4 is at the basis of the successful controller of Figure 3. Further, the two DO peaks at samples 1500 and 3400 correspond to an increased organic load, as reflected by the two N_{tot} peaks.
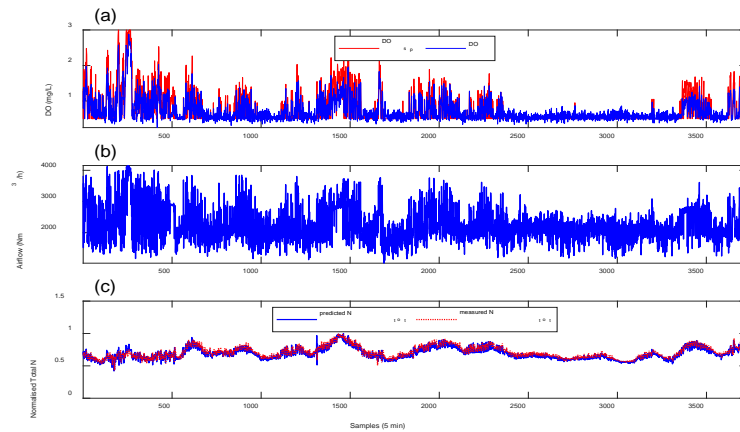
Figure 8. Output process variables during a high-load test period during which the output quality was optimised. (a) DO vs. DO set-point; (b) Airflow; (c) Comparison between predicted and measured total N (normalised).
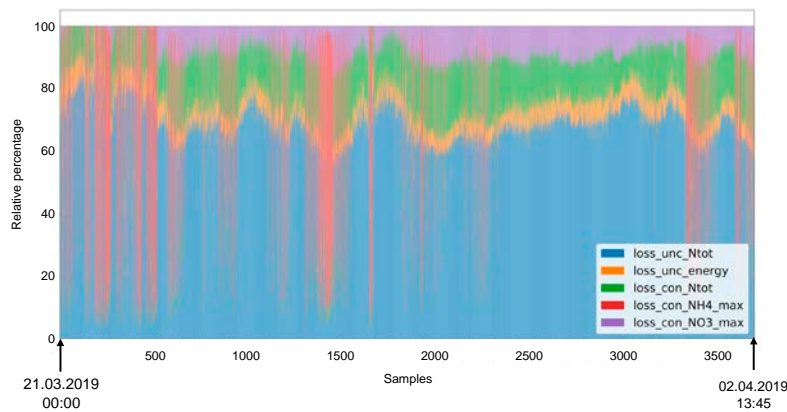
Figure 9 Relative weights in the loss function eq. (1) during the run of Figure 8.

Figure 9 shows the relative weights of the loss function during the quality effluent optimisation. The blue bars, corresponding to the unconstrained N_{tot} term, are comparatively larger than any other one, indicating that the emphasis is primarily placed on the minimisation of the output Nitrogen. The green bars show that the further constraint on N_{tot}^* is also activated most of the time, because the Nitrogen values are near the high end of the allowable band.
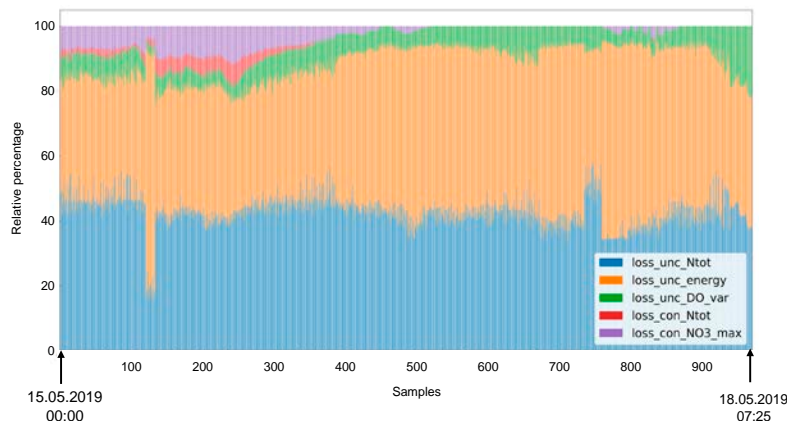
Figure 10 Relative weights in the loss function under the energy conservation objective.

Conversely, when the organic load is below its critical level the emphasis is placed on limiting the energy consumption. Figure 10 shows the new arrangement of the weights in the loss function (2) with more emphasis being placed on the unconstrained energy term (γ_2), while the variable weights (ρ_1, ρ_2, ρ_3) are never engaged, given the low value of the organic load.

From the previous performance figures it can be seen that the controller is able to switch between these two operational modes and selects the objective to be pursued depending on the incoming load estimated by the predictor of Figure 3. In fact, the two loss functions of Figure 9 and Figure 10 were produced at different times by the same controller which dynamically adapts its objective function depending on the present and predicted loading conditions. As shown, during high-load periods the emphasis is placed on the output quality, while in low-load condition energy conservation becomes the main goal. A blend of these two objectives is achieved by the comprehensive loss function (2) where the variable weights (ρ_1, ρ_2, ρ_3) contribute to the optimal target only under certain circumstances.

Conclusions

This paper has described the design and field testing of the EW MPC based on neuro-fuzzy networks and heuristic search. Its key aspect is the ability to predict sufficiently in advance ($\alpha > 30$ min) the N_{tot} peaks, thus anticipating the required values of dissolved oxygen and air flow to secure safe effluent standards and thus saving energy and improving the effluent quality. The forecast performances of the neuro fuzzy models obtained during the offline test were also maintained during closed-loop real-time operation, as shown in Figure 8c.

During the initial test the two controllers (EW and CC) were alternatively engaged as shown in Figure 7. The good performance obtained with EW controller (Table 1) with respect to the two management goals (effluent quality and energy conservation) eventually led to the decision of adopting the EW controller on a permanent basis. The flexibility of the controller is also demonstrated by comparing the relative weights of the loss function (2) in two periods with differing treatment requirements, as demonstrated in Figure 9 and Figure 10. The system is presently in operation at the plant described, where it has replaced the previous conventional controller.

Acknowledgement

References

Bartoletti, N., Casagli, F., Marsili-Libelli, S., Nardi, A., and Palandri, L., 2018. Data-driven rainfall/runoff modelling based on a neuro-fuzzy inference system. *Environmental Modelling and Software*, **106**, 35–47.

Flores, X., Bonmatí, A., Poch, M., Roda, I. R., Jiménez, L., and Bañares-Alcántara, R., 2007. Multicriteria evaluation tools to support the conceptual design of activated sludge systems. *Water Science & Technology*, **56**, 85–94.

Foscoliano, C., Del Vigo, S., Mulas, M., and Tronci, S., 2016. Predictive control of an activated sludge process for long term operation. *Chemical Engineering Journal*, **304**, 1031–1044.

Francisco, M., Skogestad, S., and Vega, P., 2015. Model predictive control for the self-optimized

operation in wastewater treatment plants: Analysis of dynamic issues. *Computers and Chemical Engineering*, **82**, 259–272.

Goldar, A., Revollar, S. R., Lamanna, R., and Vega, P., 2016. Neural NLMPC schemes for the control of the activated sludge process. In: *IFAC-PapersOnLine*. 913–918.

Haimi, H., Mulas, M., Corona, F., Marsili-Libelli, S., Lindell, P., Heinonen, M., and Vahala, R., 2016. Adaptive data-derived anomaly detection in the activated sludge process of a large-scale wastewater treatment plant. *Engineering Applications of Artificial Intelligence*, **52**, 65–80.

Hakanen, J., Sahlstedt, K., and Miettinen, K., 2013. Wastewater treatment plant design and operation under multiple conflicting objective functions. *Environmental Modelling and Software*, **46**, 240–249.

Han, H. G., Qian, H. H., and Qiao, J. F., 2014. Nonlinear multiobjective model-predictive control scheme for wastewater treatment process. *Journal of Process Control*, **24**, 47–59.

Han, H. G., Zhang, L., and Qiao, J. F., 2017. Data-Based Predictive Control for Wastewater Treatment Process. *IEEE Access*, **6**, 1498–1512.

Han, H. and Qiao, J., 2014. Nonlinear model-predictive control for industrial processes: An application to wastewater treatment process. *IEEE Transactions on Industrial Electronics*, **61**, 1970–1982.

Holenda, B., Domokos, E., Rédey, Á., and Fazakas, J., 2008. Dissolved oxygen control of the activated sludge wastewater treatment process using model predictive control. *Computers and Chemical Engineering*, **32**, 1270–1278.

Hong, Y. S. and Bhamidimarri, R., 2003. Evolutionary self-organising modelling of a municipal wastewater treatment plant. *Water Research*, **37**, 1199–1212.

Jang, J. R., 1993. ANFIS : Adaptive-Network-Based Fuzzy Inference System. *IEEE Trans. on Systems, Man, and Cibernetics*, **23**, 665–685.

Jang, J. R. S., Sun, C. T., Mizutani, E., and Ho, Y., 1998. Neuro-Fuzzy and Soft Computing--A Computational Approach to Learning and Machine Intelligence. *Proceedings of the IEEE*, **86**, 600–603.

Marsili-Libelli, S., 2016. *Environmental Systems Analysis with MATLAB*, CRC Press, Boca Raton, FL., USA, pp. 546.

Marsili-Libelli, S. and Giunti, L., 2002. Fuzzy predictive control for nitrogen removal in biological wastewater treatment. *Water science and technology : a journal of the International Association on Water Pollution Research*, **45**, 37–44.

Mulas, M., Tronci, S., Corona, F., Haimi, H., Lindell, P., Heinonen, M., Vahala, R., and Baratti, R., 2013. *An application of predictive control to the Viikinmäki wastewater treatment plant*, IFAC, pp. 18-23.

Mulas, M., Tronci, S., Corona, F., Haimi, H., Lindell, P., Heinonen, M., Vahala, R., and Baratti, R., 2015. Predictive control of an activated sludge process: An application to the Viikinm??ki wastewater treatment plant. *Journal of Process Control*, **35**.

Mustapha, M. A., Manan, Z. A., and Wan Alwi, S. R., 2018. A new quantitative overall environmental performance indicator for a wastewater treatment plant. *Journal of Cleaner Production*, **167**, 815–823.

O'Brien, M., Mack, J., Lennox, B., Lovett, D., and Wall, A., 2011. Model predictive control of an activated sludge process: A case study. *Control Engineering Practice*, **19**, 54–61.

Qiao, J. F., Hou, Y., Zhang, L., and Han, H. G., 2018. Adaptive fuzzy neural network control of wastewater treatment process with multiobjective operation. *Neurocomputing*, **275**, 383–393.

Torregrossa, D., Hernández-Sancho, F., Hansen, J., Cornelissen, A., Popov, T., and Schutz, G., 2018. Energy saving in wastewater treatment plants: A plant-generic cooperative decision support system. *Journal of Cleaner Production*, **167**, 601–609.

Yang, T., Qiu, W., Ma, Y., Chadli, M., and Zhang, L., 2014. Fuzzy model-based predictive control of dissolved oxygen in activated sludge processes. *Neurocomputing*, **136**, 88–95.